d-wave bond-order charge excitations in electron-doped cuprates

2015 EPL 111 57005

(http://iopscience.iop.org/0295-5075/111/5/57005)

A Letters Journal Exploring the Frontiers of Physics

September 2015

EPL, **111** (2015) 57005
doi: 10.1209/0295-5075/111/57005

www.epljournal.org

d-wave bond-order charge excitations in electron-doped cuprates

Hiroyuki Yamase[1], Matías Bejas[2] and Andrés Greco[2]

[1] *National Institute for Materials Science - Tsukuba 305-0047, Japan*
[2] *Facultad de Ciencias Exactas, Ingeniería y Agrimensura and Instituto de Física Rosario (UNR-CONICET) Avenida Pellegrini 250, 2000 Rosario, Argentina*

received 19 June 2015; accepted in final form 28 August 2015
published online 28 September 2015

PACS 74.72.Ek – Cuprate superconductors: Electron-doped
PACS 75.25.Dk – Orbital, charge, and other orders, including coupling of these orders
PACS 78.70.Ck – X-ray scattering

Abstract – We study charge excitation spectra in the two-dimensional t-J model on a square lattice to explore a charge-order tendency recently found in electron-doped cuprates around the carrier density 0.15. The static susceptibility of d-wave charge density, which corresponds to the nematic susceptibility at the momentum transfer $\mathbf{q} = (0, 0)$, shows two characteristic peaks at momenta of the form $\mathbf{q}_1 = (q', q')$ and $\mathbf{q}_2 = (q, 0)$. These two peaks originate from the so-called $2k_F$ scattering processes enhanced by the d-wave character of the bond-charge density. The peak at $\mathbf{q}_1$ is much broader, but develops to be very sharp in the vicinity of its instability, whereas the peak at $\mathbf{q}_2$ becomes sharper with decreasing temperature, but does not diverge. The equal-time correlation function, which is measured by resonant x-ray scattering, exhibits a momentum dependence similar to the static susceptibility. We also present energy-resolved charge excitation spectra. The spectra show a V-shaped structure around $\mathbf{q} = (0, 0)$ and bend back toward close-to-zero energy due to the charge-order tendency at $\mathbf{q}_1$ and $\mathbf{q}_2$. The resulting spectra form gap-like features with a maximal gap at $\mathbf{q} \approx \mathbf{q}_1/2$ and $\mathbf{q}_2/2$. We discuss implications for the recent experiments in electron-doped cuprates.

Introduction. – Charge order (CO) in high-temperature cuprate superconductors attracts renewed interest. CO is known in La-based materials as a spin-charge stripe order [1], in which CO is accompanied by a spin order. However, a different type of CO has been observed recently in various hole-doped cuprates such as Y- [2–8], Bi- [9–11], and Hg-based [12] materials. In these materials, the CO is not accompanied by a spin order. Furthermore a modulation vector of the CO decreases with doping, the opposite tendency observed in the La-based materials. The origin of the newly found CO as well as its relation to superconductivity is under active debate [13–17].

Research interest also goes to electron-doped cuprates. Resonant inelastic x-ray scattering (RIXS) reveals that charge excitation spectra develop to form a V-shaped dispersion [18] around the momentum $\mathbf{q} = (0, 0)$ and extends up to around 1.5 eV at $\mathbf{q} = (0.6\pi, 0)$ and $(0.6\pi, 0.6\pi)$ [19] in $Nd_{2-x}Ce_xCuO_4$ with $x = 0.15$. Quite recently resonant x-ray scattering (RXS), which integrates a RIXS spectrum up to infinity with respect to energy, has revealed a charge excitation peak at $\mathbf{q} \approx (0.48\pi, 0)$ near $x = 0.15$ [20]. The observed wave vector is rather close to that found in hole-doped cuprates [2–12], implying a possible universal phenomenon for the CO in cuprate superconductors. The correlation length of the CO is, however, estimated to be 4–7 lattice constants, *i.e.*, it is not a long-range order [20].

The wave vector of $\mathbf{q} \approx (0.48\pi, 0)$ obtained by RXS [20] is covered by the RIXS by Ishii *et al.* [19], but the observed RIXS spectra do not seem to clearly suggest some characteristic feature associated with a CO, such as softening of the spectrum toward a long-range order at the corresponding wave vector. This peculiar situation motivates us to study charge excitations in electron-doped cuprates more closely from a theoretical point of view.

Charge excitations in electron-doped cuprates are not much known theoretically. Ishii *et al.* studied the usual density-density correlation functions and discussed the RIXS spectra [19]. Bejas *et al.* [21], on the other hand, studied all possible COs in the t-J model with parameters appropriate for electron-doped cuprates. They found that instead of a usual charge-order instability, various types of bond order tend to occur much more strongly. In particular, a d-wave bond-order tendency is dominant in a moderate doping region. While its instability is expected at a wave vector close to (π, π), they found a meta-stable solution of

the d-wave bond order at $\mathbf{q} \approx (0.49\pi, 0)$. This wave vector is very close to the experimental observation by RXS [20].

Encouraged by this agreement with the experiment, we study charge excitations associated with a d-wave bond order in the two-dimensional t-J model on a square lattice by taking parameters appropriate for electron-doped cuprates. We compute three quantities: static d-wave bond-order susceptibility $\chi_d(\mathbf{q}, 0)$, its spectral weight $\mathrm{Im}\chi_d(\mathbf{q}, \omega)$, and the corresponding equal-time correlation function $S(\mathbf{q})$. The second and third quantities can be measured directly by RIXS and RXS, respectively. Our obtained results capture essential features observed in experiments such as a V-shape dispersion of $\mathrm{Im}\chi_d(\mathbf{q}, \omega)$ near $\mathbf{q} = (0, 0)$ [18,19] and a short-range CO with $\mathbf{q} \approx (0.48\pi, 0)$ [20]. In addition, we obtain several new insights: First, a CO is expected also at $\mathbf{q}_1 = (q', q')$ with $q' \approx 0.84\pi$. In fact this CO has a stronger intensity than the CO at $\mathbf{q}_2 = (q, 0)$ with $q \approx 0.49\pi$. However, the peak at $\mathbf{q}_1$ is much broader in momentum space than that at $\mathbf{q}_2$ and becomes sharp only in the vicinity of its instability. Second, the dispersive peak of $\mathrm{Im}\chi_d(\mathbf{q}, \omega)$ bends back toward close-to-zero energy at $\mathbf{q}_1$ and $\mathbf{q}_2$ where $\chi_d(\mathbf{q}, 0)$ and $S(\mathbf{q})$ exhibit a peak. The resulting charge excitation spectra show gap-like features between $\mathbf{q}_1$ and $\mathbf{q} = (0, 0)$, and between $\mathbf{q} = (0, 0)$ and $\mathbf{q}_2$, with a maximal gap at $\mathbf{q} \approx \frac{1}{2}\mathbf{q}_1$ and $\frac{1}{2}\mathbf{q}_2$.

Model and formalism. – Various approximations to the t-J [21–23] and the strong coupling Hubbard [24] model show that the models have a strong tendency toward phase separation, especially for parameters appropriate for electron-doped cuprates. The phase separation, however, can be an artifact caused by neglecting the long-range Coulomb interaction. In fact, the Coulomb interaction term appears naturally when the t-J model is derived from the three-band Hubbard model [25]. Hence we include the nearest-neighbor Coulomb interaction in the t-J model as a minimal model to study electron-doped cuprates. Our model then reads

$$H = -\sum_{i,j,\sigma} t_{ij} \tilde{c}^{\dagger}_{i\sigma} \tilde{c}_{j\sigma} + J \sum_{\langle i,j \rangle} \left[\vec{S}_i \cdot \vec{S}_j - \frac{1}{4} n_i n_j \right] + V \sum_{\langle i,j \rangle} n_i n_j, \tag{1}$$

where $t_{ij} = t$ (t') is the hopping between the first (second) nearest-neighbor sites on a square lattice, J and V are the exchange and Coulomb interactions between the nearest-neighbor sites, respectively. $\langle i, j \rangle$ indicates a nearest-neighbor pair of sites. $\tilde{c}^{\dagger}_{i\sigma}$ ($\tilde{c}_{i\sigma}$) is the creation (annihilation) operator of electrons with spin σ ($\sigma = \downarrow, \uparrow$) in the Fock space without any double occupancy. $n_i = \sum_{\sigma} \tilde{c}^{\dagger}_{i\sigma} \tilde{c}_{i\sigma}$ is the electron density operator and $\vec{S}_i$ is the spin operator. The role of the V-term turns out to merely suppress phase separation in a doping and temperature (T) range relevant to cuprates. In fact, our obtained results are not affected essentially by the V-term.

In leading order of a $1/N$-expansion [26], the kinetic term of the electrons is characterized by an effective electronic dispersion

$$\varepsilon_{\mathbf{k}} = -2 \left[t \frac{\delta}{2} + J\Delta \right] (\cos k_x + \cos k_y) - 4t' \frac{\delta}{2} \cos k_x \cos k_y - \mu, \tag{2}$$

where δ is the doping rate away from half-filling and μ is the chemical potential. The bare hopping integrals t and t' are renormalized by a factor of δ. The term $J\Delta$ in eq. (2), which is not present at bare level, comes from the exchange term (the second term in eq. (1)). The magnitude of Δ describes a bond amplitude between the nearest neighbor sites. Values of Δ and μ are determined self-consistently at a given δ by solving the following equations:

$$\Delta = \frac{1}{4N_s} \sum_{\mathbf{k}} (\cos k_x + \cos k_y) n_F(\varepsilon_{\mathbf{k}}) \tag{3}$$

and

$$1 - \delta = \frac{2}{N_s} \sum_{\mathbf{k}} n_F(\varepsilon_{\mathbf{k}}). \tag{4}$$

Here n_F is the Fermi function and N_s the total number of lattice sites.

In the above scheme Bejas *et al.* studied all possible charge instabilities for both hole-doped [17] and electron-doped [21] cuprates. They found that a relevant instability to discuss the electron-doped cuprates around $\delta = 0.15$ is a d-wave bond order where bond amplitude is modulated along both x- and y-direction, and its relative phase is in antiphase[1]. This ordering pattern is shown in fig. 1 by choosing wave vectors close to those relevant in the present study.

In the present study, we explore closely a charge-order tendency associated with the d-wave bond order. In particular, we aim to give some insight into the charge excitations recently observed by RIXS and RXS in electron-doped cuprates from a theoretical point of view. Following [17] and [21] we focus on the effective dynamical d-wave charge susceptibility,

$$\chi_d(\mathbf{q}, \omega) = \frac{(8J\Delta^2)^{-1}}{1 - 2J\Pi(\mathbf{q}, \omega)} \tag{5}$$

which becomes exact in leading order of $1/N$. The bare polarizability $\Pi(\mathbf{q}, \omega)$ reads

$$\Pi(\mathbf{q}, \omega) = -\frac{1}{N_s} \sum_{\mathbf{k}} \gamma^2(\mathbf{k}) \frac{n_F(\epsilon_{\mathbf{k}+\mathbf{q}/2}) - n_F(\epsilon_{\mathbf{k}-\mathbf{q}/2})}{\epsilon_{\mathbf{k}+\mathbf{q}/2} - \epsilon_{\mathbf{k}-\mathbf{q}/2} - \omega - \mathrm{i}\eta}, \tag{6}$$

where $\eta (> 0)$ is an infinitesimally small value and we take $\eta = 10^{-3}$ because of a practical reason of numerical computations. The form factor $\gamma(\mathbf{k}) = (\cos k_x - \cos k_y)/2$ comes from the intra-unit-cell symmetry. This form factor has d-wave symmetry, and $\chi_d(\mathbf{q}, \omega)$ corresponds to the

[1] This order is referred to as $\mathrm{BOP}_{x\bar{y}}$ in [21].

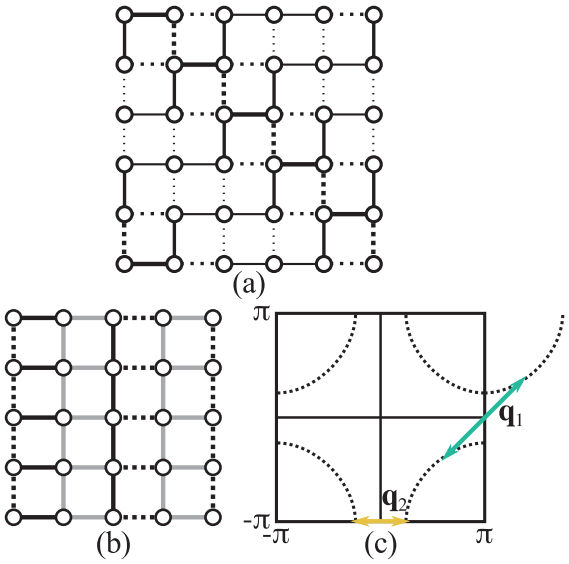

Fig. 1: (Color online) d-wave bond order for $\mathbf{q}_1 \approx \mathbf{q} = (0.8\pi, 0.8\pi)$ (a) and $\mathbf{q}_2 \approx \mathbf{q} = (0.5\pi, 0)$ (b). The black lines denote a stronger (solid line) and weaker (dotted line) bond relative to the average bond amplitude (gray line), which corresponds to Δ in eq. (3). The width of the lines indicates the modulation amplitude. (c) $2k_F$ scattering processes, which determine the wave vectors $\mathbf{q}_1$ and $\mathbf{q}_2$.

well-known nematic susceptibility for $\mathbf{q} = 0$ [27–29]. The property of $\chi_d(\mathbf{q}, \omega)$ near $\mathbf{q} = 0$ was already studied in [30] by focusing on a collective mode of the d-wave bond order in both paramagnetic and superconducting states. Here we study eq. (5) in a different situation in which COs tend to occur at $\mathbf{q} = \mathbf{q}_1$ and $\mathbf{q}_2$.

In what follows we present results for $J/t = 0.3$ and $t'/t = 0.30$, which are suitable for electron-doped cuprates. We fix the carrier density $\delta = 0.15$ so that our results will be compared directly with recent experiments [18–20]. Our conclusions do not depend sensitively on a precise choice of parameters and we choose $V/t = 1$. Below we present all quantity of the dimension of energy in units of t.

Results. – We present the static susceptibility $\chi_d(\mathbf{q}, 0)$, the equal-time correlations function $S(\mathbf{q})$, and the spectral weight $\mathrm{Im}\chi_d(\mathbf{q}, \omega)$ in $(\mathbf{q}, \omega)$ space. RXS and RIXS measure $S(\mathbf{q})$ and $\mathrm{Im}\chi_d(\mathbf{q}, \omega)$, respectively.

We first computed $\chi_d(\mathbf{q}, 0)$ in the entire Brillouin zone and found two well-defined peaks at $\mathbf{q}_1 = (0.84\pi, 0.84\pi)$ and $\mathbf{q}_2 = (0.49\pi, 0)$ near zero temperature. To clarify their temperature dependence, we plot $\chi_d(\mathbf{q}, 0)$ along the $(0,0)$-(π,π) direction in fig. 2(a). At $T = 10^{-5}$ a very sharp peak forms at $\mathbf{q} = \mathbf{q}_1$. This peak is due to the proximity to a quantum critical point of the d-wave bond-order instability, which is present at $\delta_c \approx 0.13$ [21]. However, once the temperature is increased, the peak is immediately broadened and becomes less clear already at $T = 0.01$. In fig. 2(b) we plot $\chi_d(\mathbf{q}, 0)$ along the $(0,0)$-$(\pi,0)$ direction.

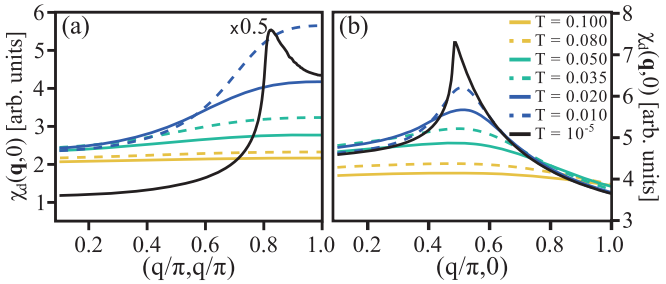

Fig. 2: (Color online) The static susceptibility $\chi_d(\mathbf{q}, 0)$ along the directions of $(0,0)$-(π,π) (a) and $(0,0)$-$(\pi,0)$ (b) for various temperatures. In (a), the curve at $T = 10^{-5}$ is scaled by a factor of 0.5.

In contrast to fig. 2(a), the temperature dependence of the peak features more usual behavior in the sense that the peak is broad at high T and smoothly grows to be a pronounced peak at low temperature. In spite of this clear peak structure, $\chi_d(\mathbf{q}, 0)$ does not diverge at $\mathbf{q}_2$. That is, there is no indication that the d-wave bond order becomes long range along the $(0,0)$-$(\pi,0)$ direction.

The static susceptibility $\chi_d(\mathbf{q}, 0)$ is a useful quantity to study the stability of a system, *i.e.*, an ordering phenomenon. This quantity is, however, not measured directly by RXS. Rather, RXS measures the equal-time correlation function $S(\mathbf{q})$, which is defined by

$$S(\mathbf{q}) = \frac{1}{\pi} \int_{-\infty}^{\infty} \mathrm{d}\omega \, \mathrm{Im}\chi_d(\mathbf{q}, \omega) \left[n_B(\omega) + 1 \right], \qquad (7)$$

where n_B is the Bose factor. In fig. 3(a) we show an intensity map of $S(\mathbf{q})$ along the $(0,0)$-(π,π) direction in a temperature range $0 < T \leq 0.1$. Although the spectral weight tends to accumulate around $\mathbf{q} = \mathbf{q}_1$ with decreasing T, the temperature dependence is weak and the spectral weight still spreads down to zero temperature in spite of the proximity of the corresponding charge instability. To show the temperature dependence of $S(\mathbf{q})$ more clearly, we plot a spectrum $\Delta S(\mathbf{q}; T) = S(\mathbf{q}; T) - S(\mathbf{q}; T = 0.1)$ in fig. 3(b). Its temperature dependence is very similar to that of the static susceptibility shown in fig. 2(a) except at $T = 10^{-5}$. In fig. 3(c) and (d), we present the corresponding results along the $(0,0)$-$(\pi,0)$ direction. Although the CO tendency is stronger at $\mathbf{q} = \mathbf{q}_1$ than at $\mathbf{q} = \mathbf{q}_2$ (see fig. 2), the peak structure at $\mathbf{q} = \mathbf{q}_2$ is much clearer, being sharp and pronounced with decreasing T, as demonstrated in fig. 3(d).

The energy-resolved spectral weight $\mathrm{Im}\chi_d(\mathbf{q}, \omega)$ is shown in fig. 4 at low temperature in the plane of $\mathbf{q}$ and ω. A V-shape dispersion develops from $\mathbf{q} = (0,0)$. This dispersion originates from individual particle-hole excitations and extends up to high energy. However, the spectrum bends back and softens toward close-to-zero energy at $\mathbf{q} = \mathbf{q}_1$ and $\mathbf{q}_2$, where both static susceptibility (fig. 2) and equal-time correlation function (fig. 3) exhibit a peak. These dispersions near $\mathbf{q}_1$ and $\mathbf{q}_2$ are interpreted as coming from collective charge excitations. This collective feature

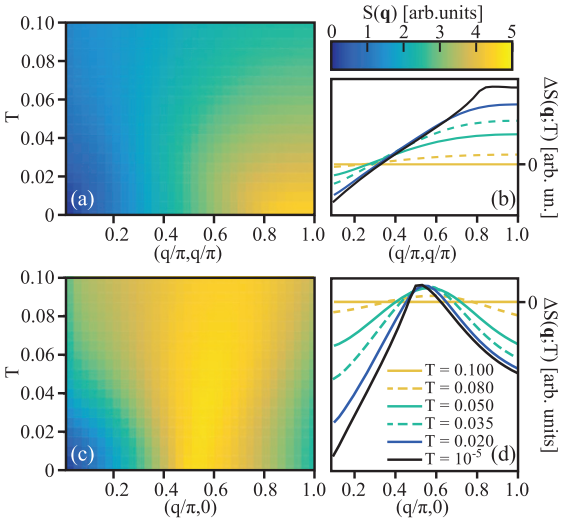

Fig. 3: (Color online) (a) Intensity map of $S(\mathbf{q})$ along the $(0,0)$-(π,π) direction for $0 < T \leq 0.1$. (b) Evolution of the spectral weight $\Delta S(\mathbf{q};T) = S(\mathbf{q};T) - S(\mathbf{q};T=0.1)$ for various temperatures. Consequently $\Delta S(\mathbf{q};T) = 0$ at $T = 0.1$. (c) and (d): results corresponding to (a) and (b), respectively, along the $(0,0)$-$(\pi,0)$ direction.

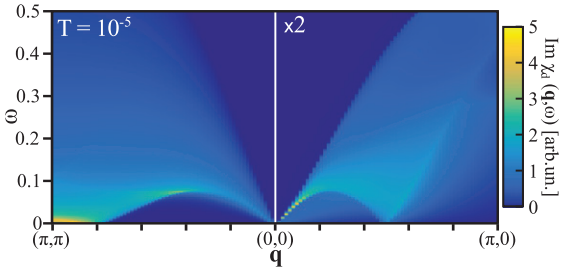

Fig. 4: (Color online) Energy-resolved spectral weight $\mathrm{Im}\chi_d(\mathbf{q},\omega)$ in the plane of $\mathbf{q}$ and ω along the symmetry axes at low temperature. The spectral weight is scaled by a factor of 2 along the $(0,0)$-$(\pi,0)$ direction to get a better contrast to that along the (π,π)-$(0,0)$ direction.

is particularly clear near $\mathbf{q} = \mathbf{q}_1$ due to the proximity to the corresponding charge instability. A gap-like feature of charge excitations is visible between $\mathbf{q}_1$ and $\mathbf{q} = (0,0)$, and also between $\mathbf{q} = (0,0)$ and $\mathbf{q}_2$, and forms a maximal gap of about 0.1 at $\mathbf{q} \approx \frac{1}{2}\mathbf{q}_1$ and $\frac{1}{2}\mathbf{q}_2$. This gap-like feature is more pronounced along the $(0,0)$-(π,π) direction because the d-wave character of the bond-charge density suppresses its low-energy scattering processes substantially.

Discussions. – Now we discuss implications for the experiments by RXS [20] and RIXS [18,19].

In fig. 3(c) and (d), the charge peak at $\mathbf{q} = \mathbf{q}_2$ becomes sharper with decreasing temperature in the equal-time correlation function, but the real part of the susceptibility remains finite at the corresponding wave vector (fig. 2(b)). We therefore conclude that the CO at $\mathbf{q} = \mathbf{q}_2$ remains a short range, which is consistent with the RXS measurements [20]. In particular, a short-range feature of the observed CO can be interpreted as an intrinsic property, *i.e.*, it does not come from some disorders frequently present in actual materials.

On the other hand, the present theory predicts that the CO tendency at $\mathbf{q} = \mathbf{q}_1$ is much stronger than at $\mathbf{q} = \mathbf{q}_2$. This is because a long-range order with modulation vector $\mathbf{q} \approx \mathbf{q}_1$ occurs at $T = 0$ at the critical doping $\delta_c \approx 0.13$ [21]. This peak at $\mathbf{q}_1$ is, however, peculiar in the sense that it is much broader than at $\mathbf{q} = \mathbf{q}_2$ and becomes sharper only in the vicinity of the charge instability. Since $\mathbf{q}_1$ is rather close to (π,π), it is not straightforward to test it in experiment. In fact, it is difficult to perform RXS and RIXS up to near (π,π). Hence a usual x-ray diffraction measurement can be more fruitful by exploring lattice modulations generated by the underlaying CO. Given that the CO instability at $\mathbf{q} \approx \mathbf{q}_1$ is expected below $\delta \lesssim \delta_c$ [21], it might seem easier to measure a sample with lower carrier density than 0.15. However, antiferromagnetism tends to be stabilized at lower carrier density and could mask the CO instability.

The peak positions at $\mathbf{q}_1$ and $\mathbf{q}_2$ found in $\chi_d(\mathbf{q},0)$ (fig. 2) and $S(\mathbf{q})$ (fig. 3) are determined mainly by two factors: the so-called $2k_F$ scattering processes [31] and the d-wave character of the bond order. The corresponding scattering processes are depicted in fig. 1(c). In particular, the peak at $\mathbf{q}_2$ becomes pronounced substantially by the d-wave form factor. Hence we expect that the observed CO at $\mathbf{q} = \mathbf{q}_2$ [20] has a d-wave character, which may be tested by RXS in the future [32].

As shown in fig. 4, charge excitations feature a V-shaped spectrum around $\mathbf{q} = (0,0)$, which agrees qualitatively with the experimental observations [18,19]. The spectra near $\mathbf{q} = (0,0)$ come mainly from individual particle-hole excitations, in favor of the experimental interpretation by Ishii *et al.* [19]. A quantitative comparison with the experiment requires additional care. The V-shaped dispersion reported in [19] extends to 1.5 eV at $\mathbf{q} = (0.6\pi,0)$ and $(0.6\pi,0.6\pi)$. Using $t/2 = 500$ meV (see footnote [2]), which is the estimated value for cuprates [33], our obtained dispersion (fig. 4) extends up to $\omega \approx 500$ meV at the same momenta. This energy scale is about a factor of three lower than the experimental observation. Our small energy scale originates mainly from a relatively small band width due to the renormalization of the bare t to an effective hopping $t_{\mathrm{eff}} = t\delta$, as seen in eq. (2). On the other hand, a large band width develops immediately after doping the Mott insulator phase, which cannot be captured quantitatively in terms of t_{eff}. In this sense, a quantitative comparison of energy scale of charge excitations is connected with a fundamental issue of doped Mott insulators and remains to be studied. Furthermore in present study we focus on charge excitations of d-wave bond order because it gives the most relevant contributions to charge excitations at low energy. For a full comparison with RIXS

[2] A factor of 1/2 here comes from a large-N formalism, where t is scaled by $1/N$. We may then invoke $N = 2$ when making a comparison with experiment.

data, however, charge excitations from other types of bond orders [21] as well as the usual charge density should be considered since RIXS may contain spectra of those excitations especially in a high energy region. At low energy, contributions from the d-wave bond order should become dominant and thus it is interesting to test a softening of charge excitation spectrum at $\mathbf{q}_1$ and $\mathbf{q}_2$ (see fig. 4) by RIXS and to clarify the actual energy scale there.

The square lattice in the present model describes the Cu sites in the CuO_2 plane of cuprate superconductors and the center of the nearest-neighbor sites corresponds to the oxygen site. Therefore our bond order may be interpreted as a charge modulation at the oxygen sites [32].

It is natural to consider whether the present theory can be applied also to hole-doped cuprates by taking appropriate parameters. Comprehensive calculations in the hole-doped case [17], however, did not capture a CO tendency compatible to the experimental observation [2–12]. Such calculations were performed in the paramagnetic state whereas in reality the CO is observed as an instability in the pseudogap state. Hence we consider that the effect of the pseudogap is crucial to understand the origin of the CO in hole-doped cuprates. In electron-doped cuprates, on the other hand, the CO tendency is observed in the paramagnetic state[3]. This may be a reason why the present theory works for that case.

While we have assumed the paramagnetic state, one may wonder whether the present theoretical framework actually predicts the strong asymmetry of the pseudogap between electron-doped cuprates ($t' > 0$) and hole-doped cuprates ($t' < 0$) simply by taking a different sign of t'. The origin of the pseudogap remains controversial even in hole-doped cuprates [35,36]. If one assumes that the pseudogap is driven by a strong charge-order tendency as hinted in some experiments [37–40], a theoretical study [21] using the present large-N scheme indeed suggests that pseudogap features should appear much weaker in electron-doped cuprates than hole-doped cuprates in the sense that a charge-order tendency becomes much weaker in the former especially in a moderate doping region relevant to the pseudogap (see fig. 6 in [21]).

Summary. – Motivated by the recent measurements by RXS and RIXS in electron-doped cuprates, we have studied charge excitation spectra associated with a d-wave bond order in the two-dimensional t-J model on a square lattice. We find that the static d-wave bond-order susceptibility $\chi_d(\mathbf{q}, 0)$ has two peaks at $\mathbf{q}_1 = (0.84\pi, 0.84\pi)$ and $\mathbf{q}_2 = (0.49\pi, 0)$, which are generated by the $2k_F$ scattering processes enhanced by the d-wave character of bond-charge density. In spite of the proximity to the d-wave CO instability at $\mathbf{q} \approx \mathbf{q}_1$, the peak at $\mathbf{q}_1$ is very broad and becomes sharp only in the vicinity of its instability. On the other hand, the peak at $\mathbf{q}_2$ becomes sharper with decreasing temperature but does not diverge, indicating that the CO with momentum $\mathbf{q}_2$ is short ranged. These features are seen also in the equal-time correlation function $S(\mathbf{q})$. The spectral function of the d-wave bond order ($\mathrm{Im}\chi_d(\mathbf{q}, \omega)$) forms a V-shape dispersion near $\mathbf{q} = (0, 0)$. This dispersion comes mainly from particle-hole excitations. The spectra bend back and reach close-to-zero energy at $\mathbf{q} = \mathbf{q}_1$ and $\mathbf{q}_2$ where both the static d-wave susceptibility and the equal-time correlation function show a peak. The resulting spectra have charge gap-like features with a maximal gap at $\mathbf{q} \approx \frac{1}{2}\mathbf{q}_1$ and $\frac{1}{2}\mathbf{q}_2$. We argue that the CO observed in RXS is interpreted as a short-range order, which may not develop to become long range. It is interesting to explore gap-like features of the energy-resolved spectra and a possible CO near $\mathbf{q} \approx \mathbf{q}_1$ by RIXS and usual x-ray diffraction measurements, respectively, for electron-doped cuprates.

* * *

The authors thank M. Fujita, K. Ishii, and T. Tohyama for stimulating discussions about RXS and RIXS for electron-doped cuprates. HY acknowledges Instituto de Física Rosario (UNR-CONICET) for hospitality and support by a Grant-in-Aid for Scientific Research from Monkasho.

REFERENCES

[1] Tranquada J. M., Sternlieb B. J., Axe J. D., Nakamura Y. and Uchida S., *Nature (London)*, **375** (1995) 561.

[2] Wu T., Mayaffre H., Krämer S., Horvatić M., Berthier C., Hardy W. N., Liang R., Bonn D. A. and Julien M.-H., *Nature*, **477** (2011) 191.

[3] Ghiringhelli G., Le Tacon M., Minola M., Blanco-Canosa S., Mazzoli C., Brookes N. B., Luca G. M. D., Frano A., Hawthorn D. G., He F., Loew T., Sala M. M., Peets D. C., Salluzzo M., Schierle E., Sutarto R., Sawatzky G. A., Weschke E., Keimer B. and Braicovich L., *Science*, **337** (2012) 821.

[4] Chang J., Blackburn E., Holmes A. T., Christensen N. B., Larsen J., Mesot J., Liang R., Bonn D. A., Hardy W. N., Watenphul A., v. Zimmermann M., Forgan E. M. and Hayden S. M., *Nat. Phys.*, **8** (2012) 871.

[5] Achkar A. J., Sutarto R., Mao X., He F., Frano A., Blanco-Canosa S., Le Tacon M., Ghiringhelli G., Braicovich L., Minola M., Moretti Sala M., Mazzoli C., Liang R., Bonn D. A., Hardy W. N., Keimer B., Sawatzky G. A. and Hawthorn D. G., *Phys. Rev. Lett.*, **109** (2012) 167001.

[6] LeBoeuf D., Krämer S., Hardy W. N., Liang R., Bonn D. A. and Proust C., *Nat. Phys.*, **9** (2013) 79.

[7] Blackburn E., Chang J., Hücker M., Holmes A. T., Christensen N. B., Liang R., Bonn D. A.,

[3] Although a pseudogap was reported in the optical conductivity spectra in the non-superconducting crystals [34], the pseudogap corresponding to the observed one in hole-doped cuprates, namely a gap-like feature above the superconducting phase, is missing or at least very weak.

Hardy W. N., Rütt U., Gutowski O., v. Zimmermann M., Forgan E. M. and Hayden S. M., *Phys. Rev. Lett.*, **110** (2013) 137004.

[8] Blanco-Canosa S., Frano A., Schierle E., Porras J., Loew T., Minola M., Bluschke M., Weschke E., Keimer B. and Le Tacon M., *Phys. Rev. B*, **90** (2014) 054513.

[9] Comin R., Frano A., Yee M. M., Yoshida Y., Eisaki H., Schierle E., Weschke E., Sutarto R., He F., Soumyanarayanan A., He Y., Le Tacon M., Elfimov I. S., Hoffman J. E., Sawatzky G. A., Keimer B. and Damascelli A., *Science*, **343** (2014) 390.

[10] da Silva Neto E. H., Aynajian P., Frano A., Comin R., Schierle E., Weschke E., Gyenis A., Wen J., Schneeloch J., Xu Z., Ono S., Gu G., Le Tacon M. and Yazdani A., *Science*, **343** (2014) 393.

[11] Hashimoto M., Ghiringhelli G., Lee W.-S., Dellea G., Amorese A., Mazzoli C., Kummer K., Brookes N. B., Moritz B., Yoshida Y., Eisaki H., Hussain Z., Devereaux T. P., Shen Z.-X. and Braicovich L., *Phys. Rev. B*, **89** (2014) 220511.

[12] Tabis W., Li Y., Le Tacon M., Braicovich L., Kreyssig A., Minola M., Dellea G., Weschke E., Veit M. J., Ramazanoglu M., Goldman A. I., Schmitt T., Ghiringhelli G., Barišić N., Chan M. K., Dorow C. J., Yu G., Zhao X., Keimer B. and Greven M., *Nat. Commun.*, **5** (2014) 5875.

[13] Meier H., Pepin C., Einenkel M. and Efetov K., *Phys. Rev. B*, **89** (2014) 195115.

[14] Sachdev S. and Placa R., *Phys. Rev. Lett.*, **111** (2013) 027202.

[15] Wang Y. and Chubukov A., *Phys. Rev. B*, **90** (2014) 035149.

[16] Atkinson W., Kampf A. and Bulut S., *New J. Phys.*, **17** (2015) 013025.

[17] Bejas M., Greco A. and Yamase H., *Phys. Rev. B*, **86** (2012) 224509.

[18] Lee W. S., Lee J. J., Nowadnick E. A., Gerber S., Tabis W., Huang S. W., Strocov V. N., Motoyama E. M., Yu G., Moritz B., Huang H. Y., Wang R. P., Huang Y. B., Wu W. B., Chen C. T., Huang D. J., Greven M., Schmitt T., Shen Z. X. and Devereaux T. P., *Nat. Phys.*, **10** (2014) 883.

[19] Ishii K., Fujita M., Sasaki T., Minola M., Dellea G., Mazzoli C., Kummer K., Ghiringhelli G., Braicovich L., Tohyama T., Tsutsumi K., Sato K., Kajimoto R., Ikeuchi K., Yamada K., Yoshida M., Kurooka M. and Mizuki J., *Nat. Commun.*, **5** (2014) 3714.

[20] da Silva Neto E. H., Comin R., He F., Sutarto R., Jiang Y., Greene R. L., Sawatzky G. A. and Damascelli A., *Science*, **347** (2015) 282.

[21] Bejas M., Greco A. and Yamase H., *New J. Phys.*, **16** (2014) 123002.

[22] Gooding R. J., Vos K. J. E. and Leung P. W., *Phys. Rev. B*, **50** (1994) 12866.

[23] Martins G. B., Xavier J. C., Arrachea L. and Dagotto E., *Phys. Rev. B*, **64** (2001) R1805.

[24] Macridin A., Jarrell M. and Maier T., *Phys. Rev. B*, **74** (2006) 085104.

[25] Feiner L., Jefferson J. and Raimondi R., *Phys. Rev. B*, **53** (1996) 8751.

[26] Foussats A. and Greco A., *Phys. Rev. B*, **70** (2004) 205123.

[27] Yamase H. and Kohno H., *J. Phys. Soc. Jpn.*, **69** (2000) 332.

[28] Yamase H. and Kohno H., *J. Phys. Soc. Jpn.*, **69** (2000) 2151.

[29] Halboth C. J. and Metzner W., *Phys. Rev. Lett.*, **85** (2000) 5162.

[30] Yamase H., *Phys. Rev. Lett.*, **93** (2004) 266404.

[31] Holder T. and Metzner W., *Phys. Rev. B*, **85** (2012) 165130.

[32] Comin R., Sutarto R., He F., da Silva Neto E. H., Chauviere L., Frano A., Liang R., Hardy W. N., Bonn D. A., Yoshida Y., Eisaki H., Achkar A. J., Hawthorn D. G., Keimer B., Sawatzky G. A. and Damascelli A., *Nat. Mater.*, **14** (2015) 796.

[33] Hybertsen M. S., Stechel E. B., Schluter M. and Jennison D. R., *Phys. Rev. B*, **41** (1990) 11068.

[34] Onose Y., Taguchi Y., Ishizaka K. and Tokura Y., *Phys. Rev. Lett.*, **87** (2001) 217001.

[35] Mishra V., Chatterjee U., Campuzano J. C. and Norman M. R., *Nat. Phys.*, **10** (2014) 357.

[36] Hashimoto M., Vishik I. M., He R.-H., Devereaux T. P. and Shen Z.-X., *Nat. Phys.*, **10** (2014) 483.

[37] Tanaka K., Lee W. S., Lu D. H., Fujimori A., Fujii T., Risdiana, Terasaki I., Scalapino D. J., Devereaux T. P., Hussain Z. and Shen Z.-X., *Science*, **314** (2006) 1910.

[38] Vishik I. M., Lee W. S., He R.-H., Hashimoto M., Hussain Z., Devereaux T. P. and Shen Z.-X., *New J. Phys.*, **12** (2010) 105008.

[39] Kondo T., Hamaya Y., Palczewski A. D., Takeuchi T., Wen J. S., Xu Z. J., Gu G., Schmalian J. and Kaminski A., *Nat. Phys.*, **7** (2011) 21.

[40] Yoshida T., Hashimoto M., Vishik I. M., Shen Z.-X. and Fujimori A., *J. Phys. Soc. Jpn.*, **81** (2012) 011006.